

## Supplementary Materials for

### **New power of self-assembling carbonic anhydrase inhibitor: Short peptide–constructed nanofibers inspire hypoxic cancer therapy**

Jiayang Li, Kejian Shi, Zeinab Farhadi Sabet, Wenjiao Fu, Huige Zhou, Shaoxin Xu, Tao Liu, Min You, Mingjing Cao, Mengzhen Xu, Xuejing Cui, Bin Hu, Ying Liu, Chunying Chen\*

\*Corresponding author. Email: chenchy@nanocr.cn

Published 6 September 2019, *Sci. Adv.* **5**, eaax0937 (2019)  
DOI: 10.1126/sciadv.aax0937

#### **This PDF file includes:**

- Fig. S1. Hydrogel performances and characterizations of N-pepABS.
- Fig. S2. CA IX–related cell behaviors in MDA-MB-231 and HeLa cells.
- Fig. S3. CA IX–related endocytosis performances in MDA-MB-231.
- Fig. S4. CA IX down-regulation inhibits nanofiber endocytosis under hypoxia.
- Fig. S5. Acid vesicle injuries blocked protective autophagy in MDA-MB-231 cells.
- Fig. S6. The antihypoxic cancer cells effects of N-pepABS treatment in vivo.
- Fig. S7. Inhibition of tumor growth and metastasis on 4T1 tumor model.
- Fig. S8. In vivo toxicity evaluation after different treatments.
- Fig. S9. The synthesis and characterization of samples.

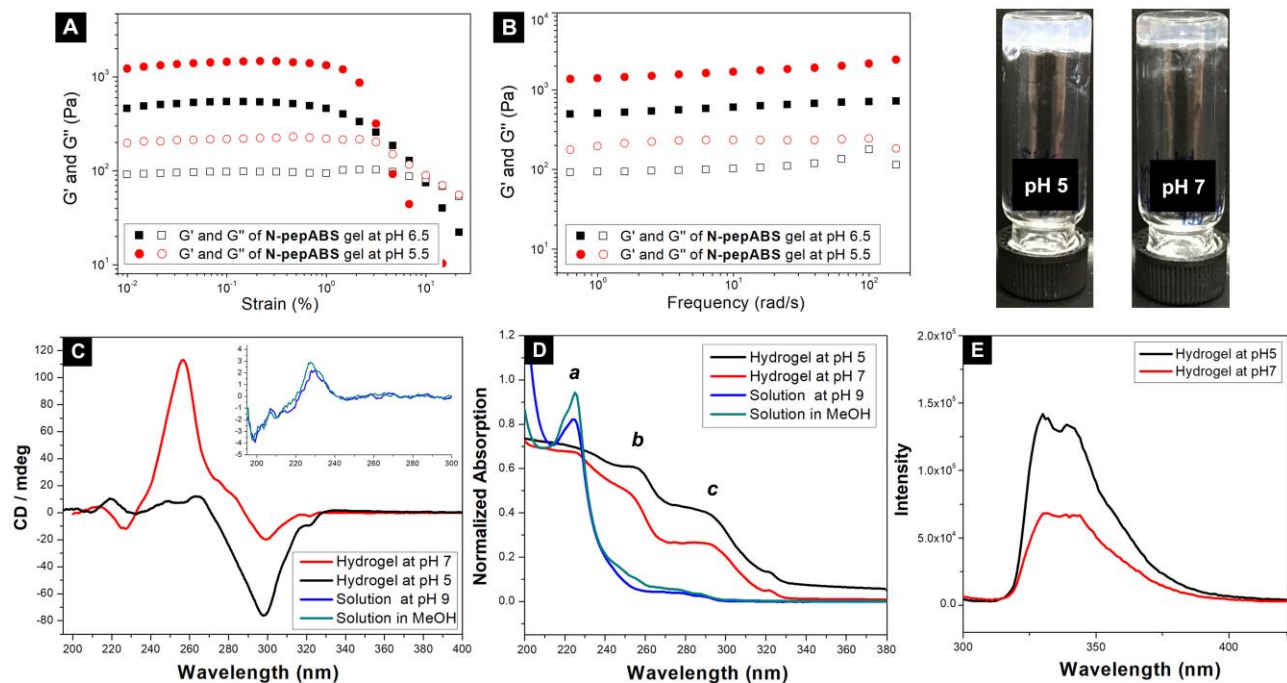


**Fig. S1. Hydrogel performances and characterizations of N-pepABS.** (A) and (B) Oscillatory rheology of hydrogels formed by 0.75 wt% of N-pepABS at pH 6.5 / pH 5.5; (C) CD, (D) UV and (E) Fluorescence spectra of N-pepABS hydrogels (0.75 wt%) at pH 5.0 / 7.0 and their diluted solutions in MeOH or ddH<sub>2</sub>O (pH 9). (Photo credit: Chunying Chen, The National Center for Nanoscience and Technology of China).

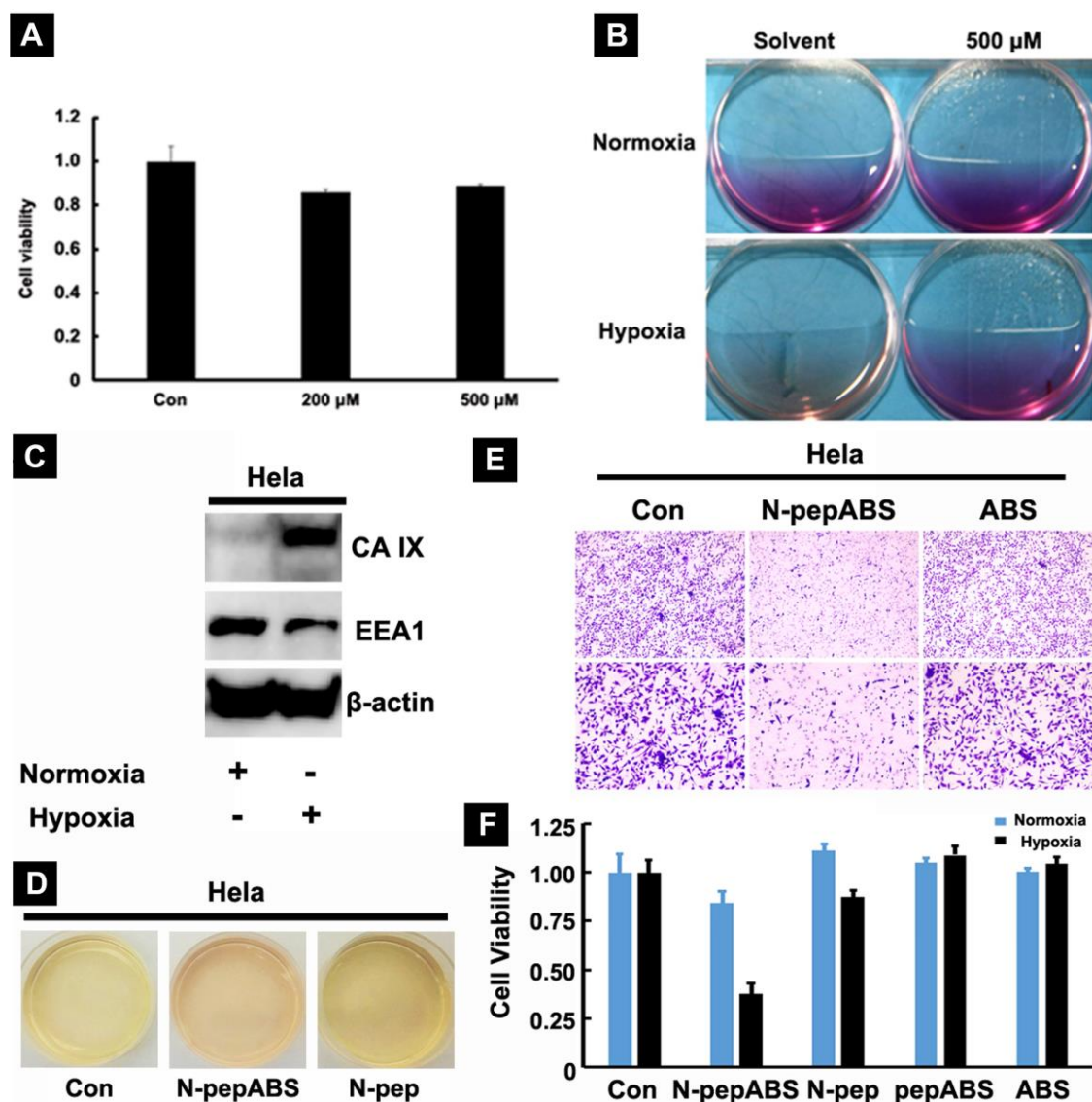


**Fig. S2. CA IX–related cell behaviors in MDA-MB-231 and HeLa cells.** (A) The cell viabilities for MDA-MB-231 cells with 24 h incubation with N-pepABS under hypoxia; (B) The optical images of the culture plates for MDA-MB-231 cells with 48 h incubation with 500  $\mu$ M of N-pepABS or solvent control under both normoxia and hypoxia. N-pepABS was a novel CA inhibitor in HeLa cells: (C) The expression of EEA1 and CA IX under normoxia or hypoxia condition (1% O<sub>2</sub>, 48 h) was evaluated with western blot experiment; (D) The alteration of medium color was observed after each treatment exposure. (E) N-pepABS could inhibit migration of HeLa cells. (F) N-pepABS selectively inhibit hypoxic HeLa cells growth in vitro. (Photo credit: Chunying Chen, The National Center for Nanoscience and Technology of China).

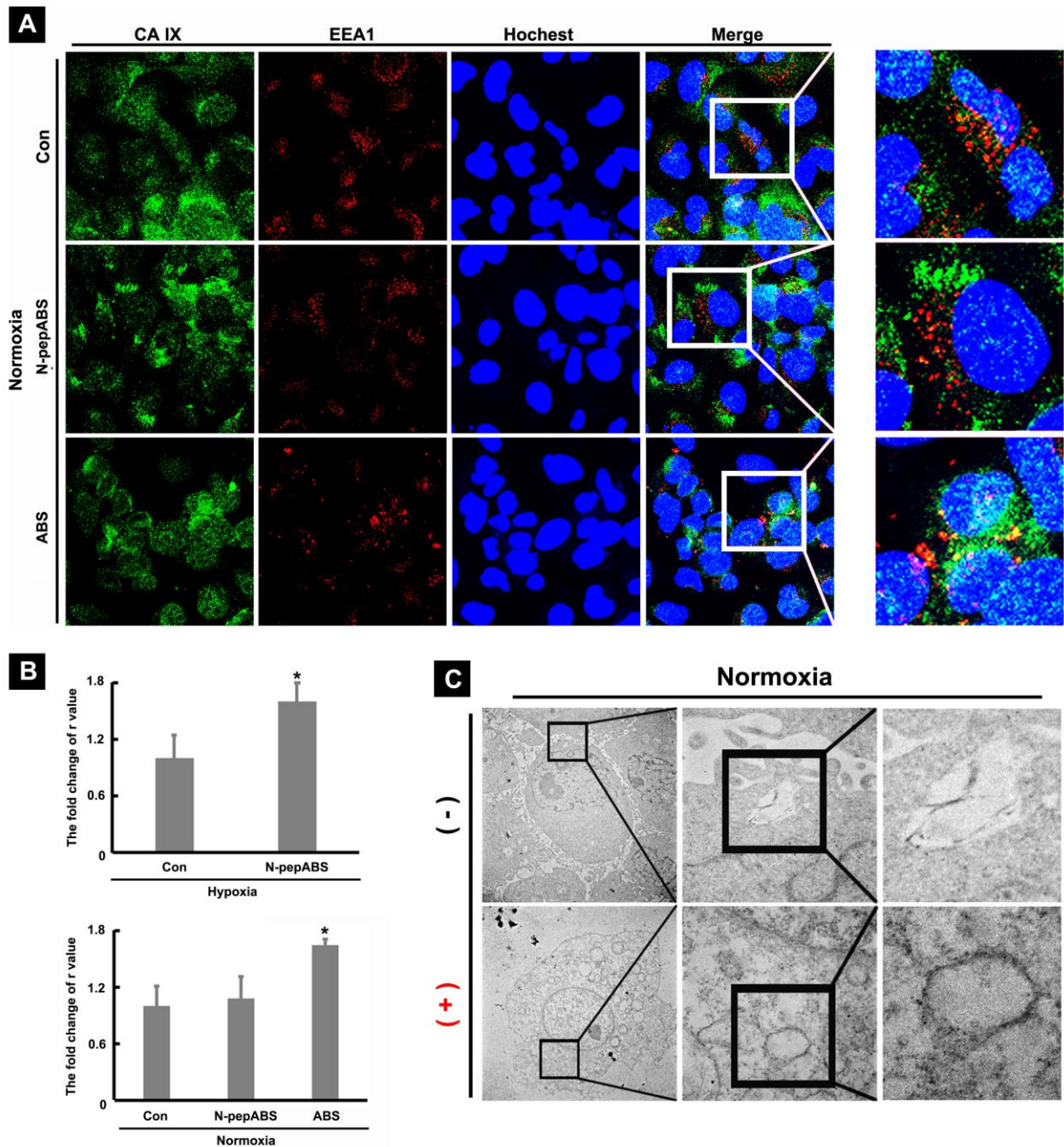


**Fig. S3. CA IX–related endocytosis performances in MDA-MB-231.** (A) Confocal images of MDA-MB-231 cells with 24 h treatment of 500  $\mu$ M ABS, N-pepABS or medium control under normoxia; (B) The fold change of R value in different treatments had been performed as a bar graph. This bar graph had been performed as mean  $\pm$  SD (n=3), while \*P<0.05 was thought as statistical significance; (C) TEM images of nanofibers in the cytoplasm of normoxic MDA-MB-231 cells, after treated with 500  $\mu$ M of N-pepABS for 48 h.

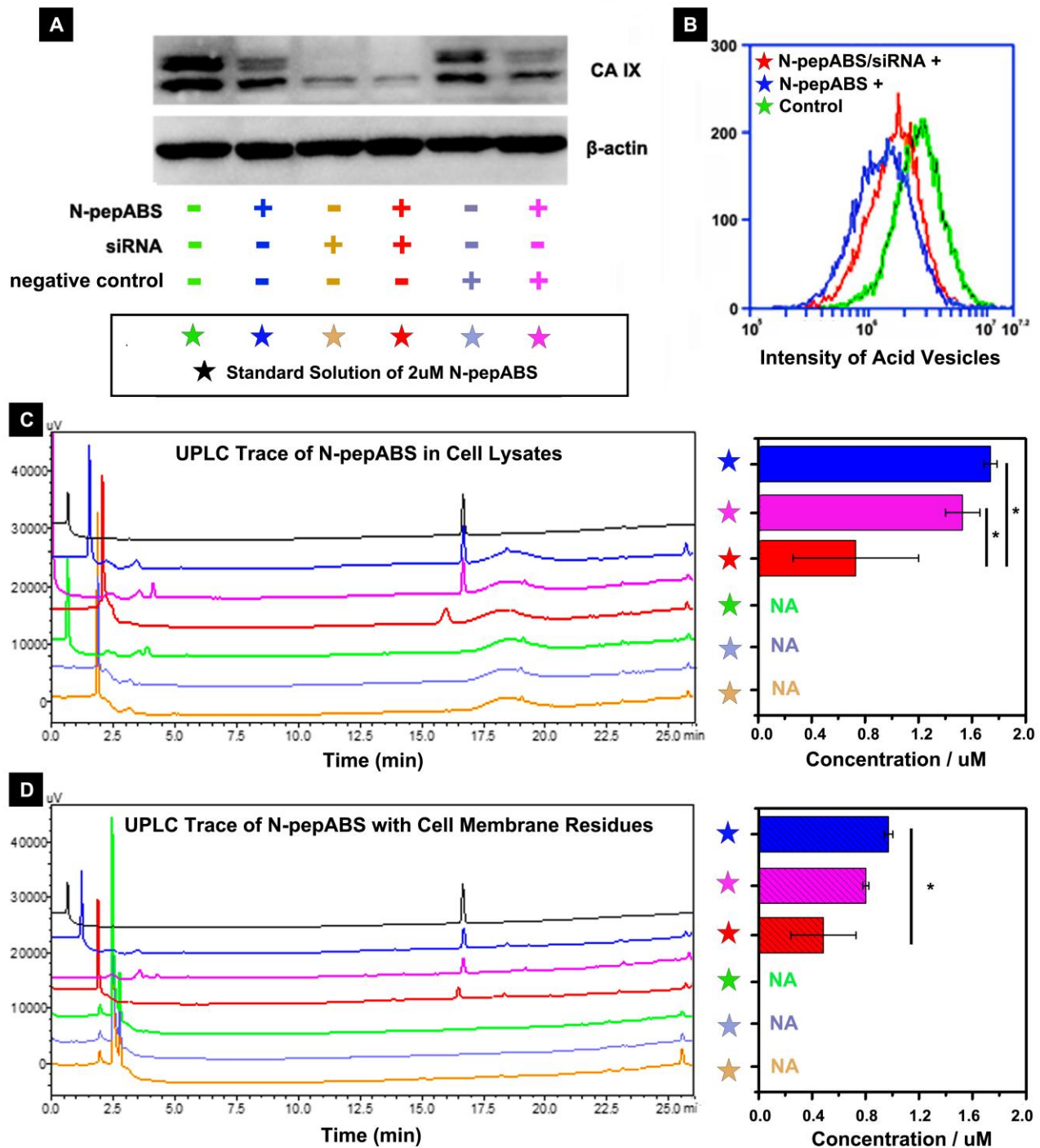


**Fig. S4. CA IX down-regulation inhibits nanofiber endocytosis under hypoxia.**

Endocytosis of the peptide was inhibited after CA IX was down-regulated: (A) Interference experiment successfully decreased CA IX expression. (B) Knockdown CA IX in hypoxic MDA-MB-231 cells could partly reverse N-pepABS induced decrease of lysosome acidity. UPLC trace of N-pepABS in (C) cell lysates and (D) in cell membrane residues with different treatments. Their corresponding concentrations was calculated and presented in the left, with bar graph performed as mean  $\pm$  SD (n=3), while \*P<0.05 was thought as statistical significance.

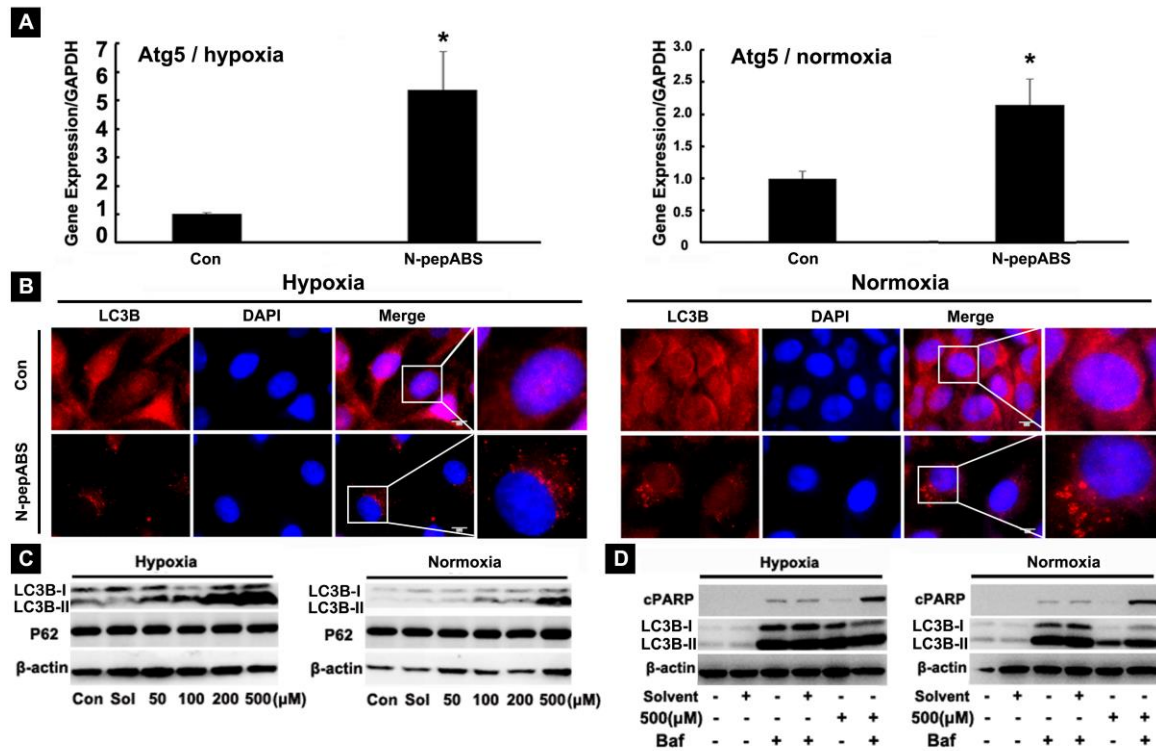


**Fig. S5. Acid vesicle injuries blocked protective autophagy in MDA-MB-231 cells.** (A) ratio of mRNA levels of Atg 5/GADPH after cells were treated with 500  $\mu$ M N-pepABS for 48 h. The bar image was represented as mean  $\pm$  SD, while \* $P < 0.05$  was thought as significant difference. (B) Fluorescent images of autophagosome accumulation in the cytoplasm of hypoxic or normoxic MDA-MB-231 cells, treated with 500  $\mu$ M N-pepABS for 48 h, with scale bar of 20  $\mu$ m. (C) Western blot assays of autophagy-related signals in MDA-MB-231 cells, treated with 500  $\mu$ M N-pepABS for 48 h; (D) Autophagy flux study in the MDA-MB-231 cells, with the pre-treatment of 10 nM Baf for 1 h and then treatment of 500  $\mu$ M N-pepABS for another 48 h.

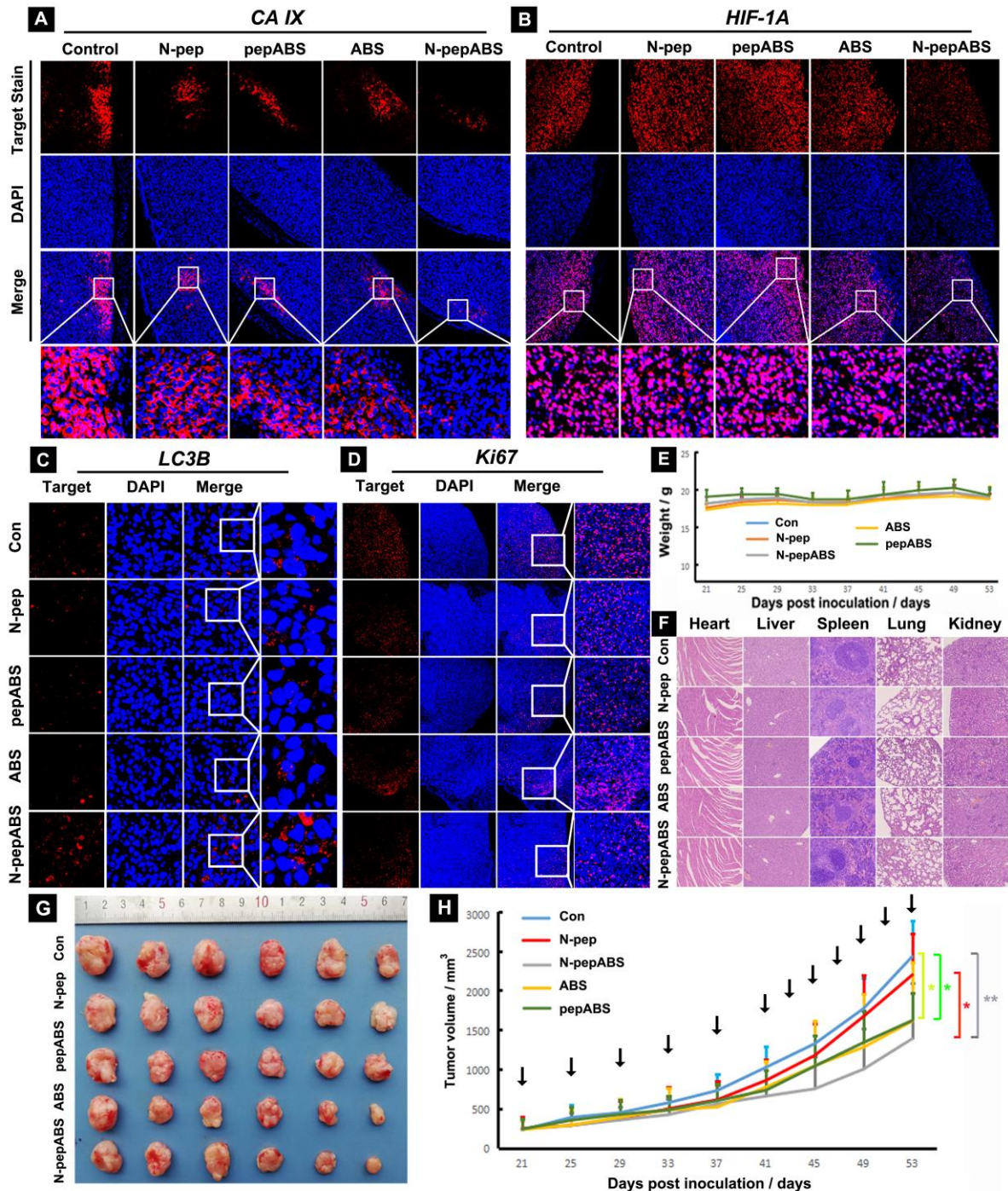


**Fig. S6. The antihypoxic cancer cells effects of N-pepABS treatment in vivo.** Alterations of (A) CA IX and (B) HIF-1 $\alpha$  expression after treatments of PBS control, N-pep, pepABS, ABS, and N-pepABS; Immunofluorescence images of (C) LC3B indicated autophagosome accumulation, as well as (D) Ki67 illuminated cell proliferation attenuation after the N-pepABS treatment; Comparing with control groups, N-pepABS treatment performs no obvious abnormality in both (E) mice weights and (F) their organs of heart, liver, spleen, lung and kidney. (G) The Optical image and (H) Tumor volume of MDA-MB-231 tumors after the treatments of N-pepABS, pepABS, N-pep, ABS, and solvent control via intratumoral injections for 20 days (every four days, 1mM, 10  $\mu$ L), then followed up with another 12 days treatment (every two days, 1mM, 10  $\mu$ L). Black arrows point out the injection days. (Photo credit: Chunying Chen, The National Center for Nanoscience and Technology of China).

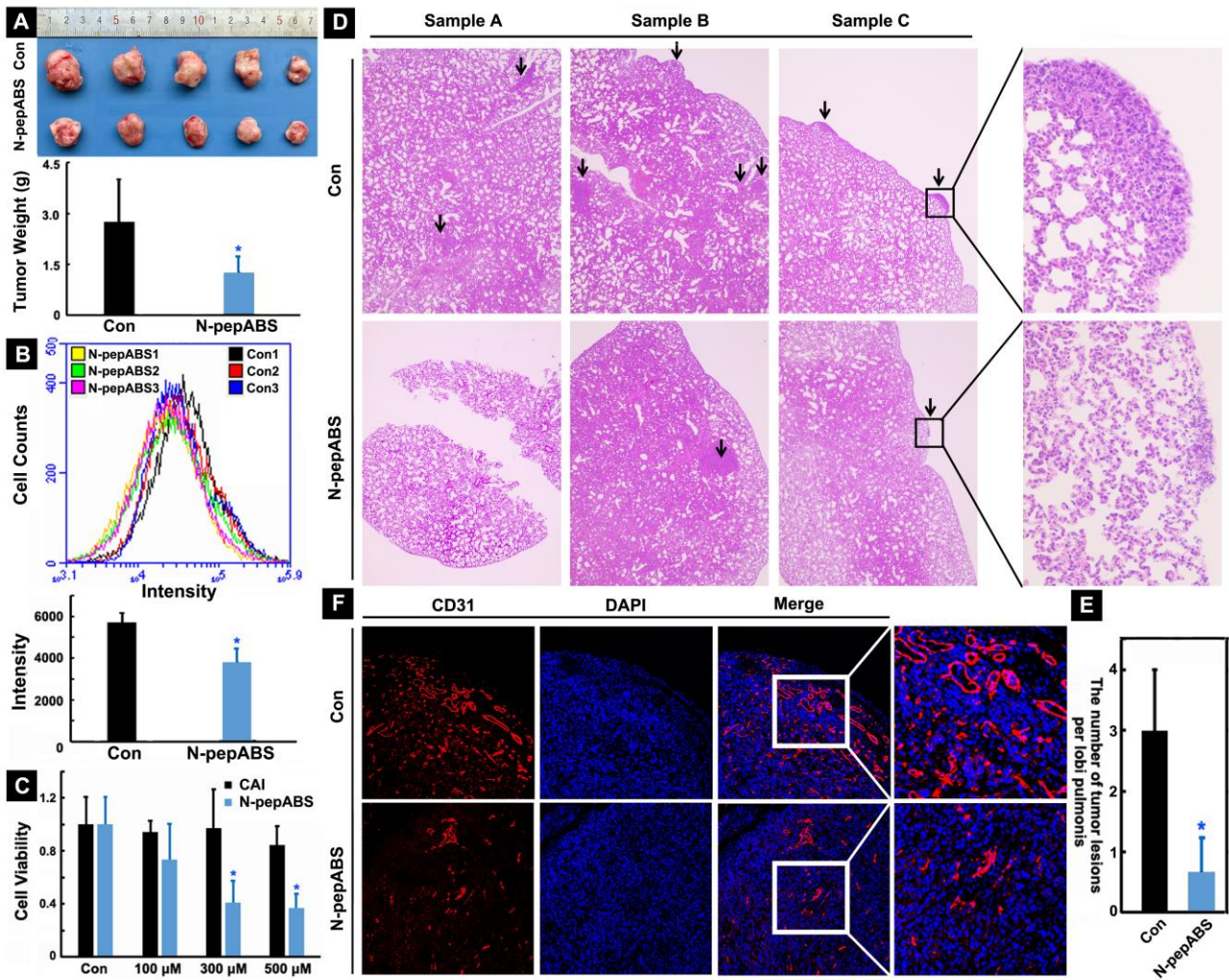


**Fig. S7. Inhibition of tumor growth and metastasis on 4T1 tumor model.** N-pepABS treatment apparently inhibits (A) tumor growth and decreases tumor weight of 4T1 cancer; (B) Flow cytometry of the expression of CA IX in tumor tissues, and the statistical analysis of their fluorescent intensity after N-pepABS treatment; (C) N-pepABS performs in vitro inhibitory effects on hypoxic 4T1 cells growth; (D) HE staining images of lung tissues with metastasis of 4T1 tumor cells from six different samples, and (E) its statistical analysis of the number of tumor lesions per lobi pulmonis; (F) Immunofluorescence images of endothelial marker CD31, indicating blood vessel variation after N-pepABS treatment. The bar graph was represented as mean  $\pm$  SD, while \* $P < 0.05$  was thought as significance. Two-tailed T tests were used to determine the different significance. (Photo credit: Chunying Chen, The National Center for Nanoscience and Technology of China).



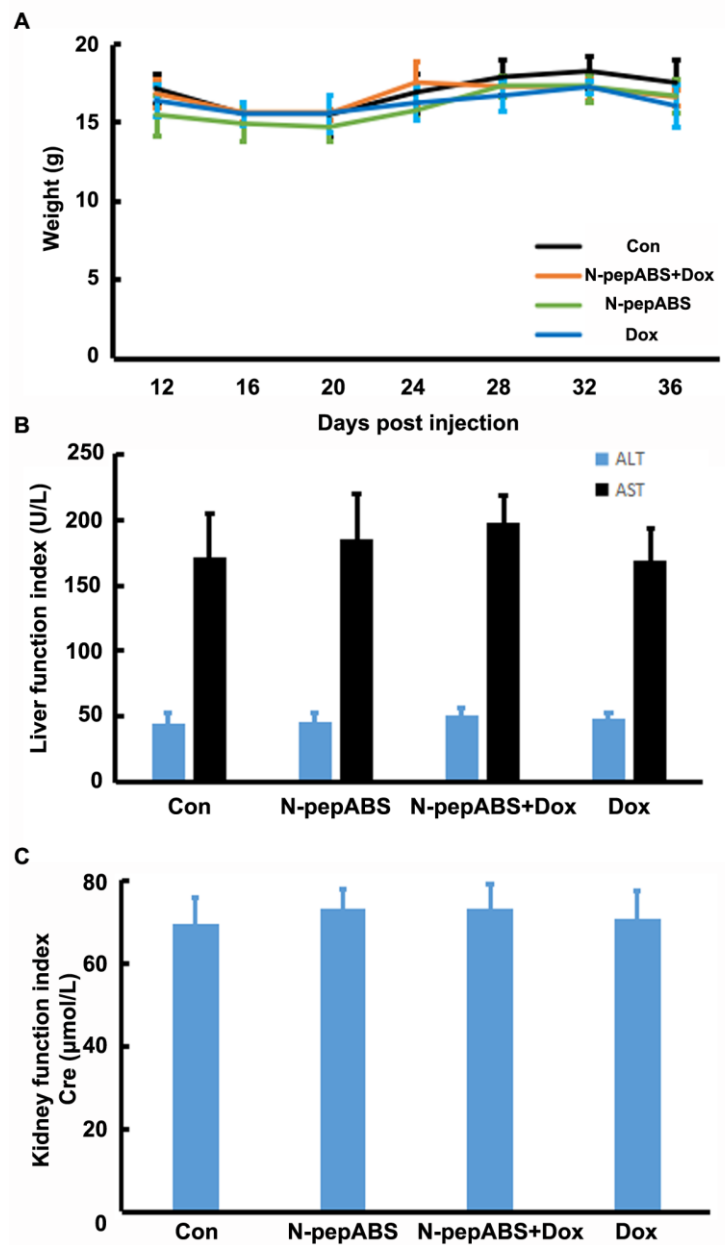


**Fig. S8. In vivo toxicity evaluation after different treatments.** Alterations of (A) body weight, (B) Alterations of liver function indexes of Alanine transaminase (ALT) and Aspartate transaminase (AST) are detected during the whole therapeutic period. (C) Alterations of kidney function index of Creatinine (Cre) are detected during the whole therapeutic period.

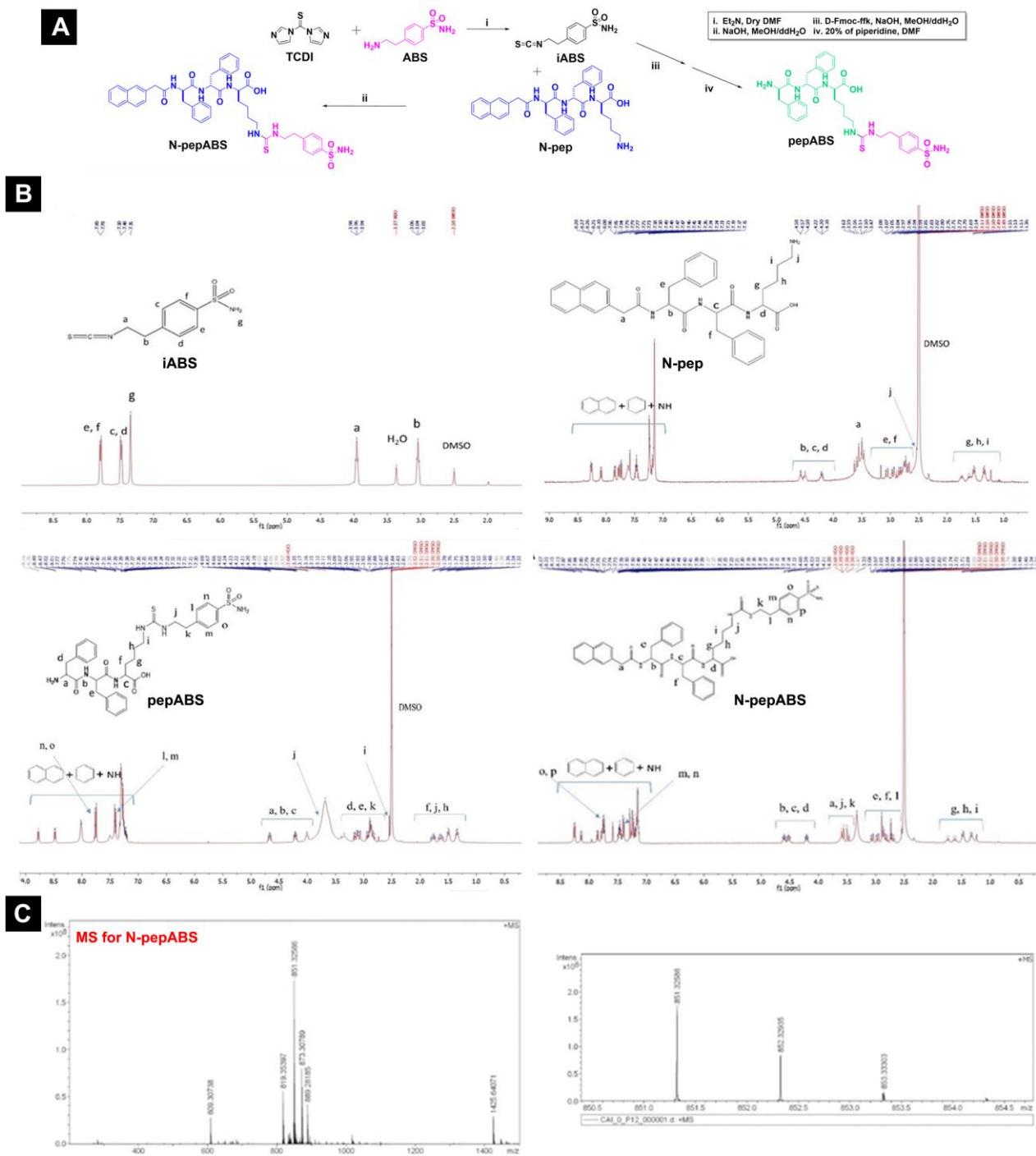


**Fig. S9. The synthesis and characterization of samples.** The synthesis route (A) and (B)  $^1\text{H}$  NMR spectrum of small molecules of N-pepABS, pepABS, iABS, N-pep in  $\text{DMSO-d}_6$ ; (B) MS spectrum of N-pepABS.